QUARTERLY JOURNAL OF THE ROYAL METEOROLOGICAL SOCIETY
Q. J. R. Meteorol. Soc. **135**: 2146–2160 (2009)
Published online 2 December 2009 in Wiley InterScience
(www.interscience.wiley.com) DOI: 10.1002/qj.526

Dynamics of nonlinear error growth and season-dependent predictability of El Niño events in the Zebiak–Cane model

Yanshan Yu,[a,b,c] Wansuo Duan,[a] Hui Xu[a] and Mu Mu[a,c]*

[a]*LASG, Institute of Atmospheric Physics, Chinese Academy of Sciences, Beijing, China*
[b]*Graduate University of Chinese Academy of Sciences, Beijing, China*
[c]*Key Laboratory of Ocean Circulation and Waves, Institute of Oceanology, Chinese Academy of Sciences, Qingdao, China*

ABSTRACT: With the intermediate-complexity Zebiak–Cane model, we investigate the 'spring predictability barrier' (SPB) problem for El Niño events by tracing the evolution of conditional nonlinear optimal perturbation (CNOP), where CNOP is superimposed on the El Niño events and acts as the initial error with the biggest negative effect on the El Niño prediction. We show that the evolution of CNOP-type errors has obvious seasonal dependence and yields a significant SPB, with the most severe occurring in predictions made before the boreal spring in the growth phase of El Niño. The CNOP-type errors can be classified into two types: one possessing a sea-surface-temperature anomaly pattern with negative anomalies in the equatorial central-western Pacific, positive anomalies in the equatorial eastern Pacific, and a thermocline depth anomaly pattern with positive anomalies along the Equator, and another with patterns almost opposite to those of the former type. In predictions through the spring in the growth phase of El Niño, the initial error with the worst effect on the prediction tends to be the latter type of CNOP error, whereas in predictions through the spring in the decaying phase, the initial error with the biggest negative effect on the prediction is inclined to be the former type of CNOP error. Although the linear singular vector (LSV)-type errors also have patterns similar to the CNOP-type errors, they cover a more localized area than the CNOP-type errors and cause a much smaller prediction error, yielding a less significant SPB. Random errors in the initial conditions are also superimposed on El Niño events to investigate the SPB. We find that, whenever the predictions start, the random errors neither exhibit an obvious season-dependent evolution nor yield a large prediction error, and thus may not be responsible for the SPB phenomenon for El Niño events. These results suggest that the occurrence of the SPB is closely related to particular initial error patterns. The two kinds of CNOP-type error are most likely to cause a significant SPB. They have opposite signs and, consequently, opposite growth behaviours, a result which may demonstrate two dynamical mechanisms of error growth related to SPB: in one case, the errors grow in a manner similar to El Niño; in the other, the errors develop with a tendency opposite to El Niño. The two types of CNOP error may be most likely to provide the information regarding the 'sensitive area' of El Niño–Southern Oscillation (ENSO) predictions. If these types of initial error exist in realistic ENSO predictions and if a target method or a data assimilation approach can filter them, the ENSO forecast skill may be improved. Copyright © 2009 Royal Meteorological Society

KEY WORDS nonlinearity; optimal perturbation

Received 22 January 2009; Revised 16 July 2009; Accepted 1 September 2009

1. Introduction

The El Niño–Southern Oscillation (ENSO) cycle, a fluctuation between unusually warm (El Niño) and cold (La Niña) conditions, is the most prominent year-to-year climate variation on Earth. Although ENSO originates and develops mainly in the tropical Pacific through interactions between the ocean and the atmosphere, its environmental and socio-economic impacts are felt worldwide. Knowledge about the ENSO cycle and the ability to forecast its variations, however limited at present, supply valuable information for agriculture, public health and safety, fisheries, forestry, and many other spheres of climate-sensitive human endeavour.

Significant progress has been made in ENSO theories and predictions over the years, especially through the TOGA (Tropical Ocean–Global Atmosphere) programme (see the review of Wang and Picaut (2004)), but there still exist considerable uncertainties in realistic ENSO predictions (Jin *et al.*, 2008; Luo *et al.*, 2008). In particular, if the forecasts are made before and through the spring, ENSO predictions tend to be much less successful. This low predictability has been related to the so-called 'spring predictability barrier' (SPB) of ENSO (Webster and Yang, 1992; Yu and Kao, 2007). SPB exists not only in coupled models but also in statistical models. Sometimes, the SPB is even stronger in statistical models than in General Circulation Models (GCMs) (van Oldenborgh *et al.*, 2005).

Many studies have explored the SPB phenomenon (Webster and Yang, 1992; Latif *et al.*, 1994; Webster, 1995; McPhaden, 2003; Mu *et al.*, 2007a, 2007b) and

*Correspondence to: Mu Mu, LASG, Institute of Atmospheric Physics, Chinese Academy of Sciences, Beijing 100029, China.
E-mail: mumu@lasg.iap.ac.cn

obtained significant results, but the debate concerning the origin of the SPB continues. One possible cause is the rapid seasonal transition of monsoon circulation during the boreal spring, a phenomenon that perturbs the Pacific's basic state when the east–west sea-surface-temperature (SST) gradient is at its weakest (Webster and Yang, 1992; Lau and Yang, 1996). Another notion, proposed by Webster (1995), is that SPB is caused by the fact that the ocean–atmosphere coupling is weakest during spring in the eastern Pacific. Other studies have argued that SST anomalies (SSTA) in the boreal spring are relatively small, making them difficult to detect and forecast in the presence of atmospheric and oceanic noise (Chen *et al.*, 1995). Samelson and Tziperman (2001) demonstrated that SPB is an inherent characteristic of ENSO, whereas Chen *et al.* (1995, 2004) suggested that improving model initialization could reduce this predictability barrier. McPhaden (2003) showed that subsurface information has a winter persistence barrier and that the predictability of ENSO across the spring can be greatly enhanced by incorporating this information into the model. Recently, Mu *et al.* (2007a) demonstrated that the SPB may result from the combined effect of the climatological mean equilibrium state, the El Niño event itself, and initial error patterns. In general, the cause of the SPB is still elusive, and there is an urgent need for our understanding of ENSO to further address the problems related to SPB.

Some papers explored the SPB by studying the transient growth of initial error. For example, Moore and Kleeman (1996) investigated the SPB by tracing the evolution of the linear singular vector (LSV: Lorenz, 1965). Blumenthal (1991), Xue *et al.* (1997), and Thompson (1998) also used the LSV approach to study ENSO predictability. In addition, Samelson and Tziperman (2001) used linear stability theory to study the SPB. All these approaches are useful in predictability studies and can be used to identify the optimal transient growth of initial perturbation in a non-self-adjoint system (Farrell, 1988; Farrell and Ioannou, 1996), but they deal with sufficiently small initial perturbations and thus are limited in describing nonlinear evolution of finite-amplitude initial perturbations (Oortwijn and Barkmeijer, 1995; Mu *et al.*, 2003).

Mu *et al.* (2007a) have used a nonlinear technique of conditional nonlinear optimal perturbation (CNOP: see section 2) as an approach to investigate the SPB for ENSO events in a theoretical model. This method tackles the evolution of finite-amplitude initial perturbation and has led to instructive results, but the model adopted is a conceptual one with only two variables, NINO-3 SSTA (the SSTA averaged over the Niño-3 region) and thermocline depth anomaly. Consequently, the spatial structure of the finite-amplitude initial errors that cause the SPB cannot be explored. Furthermore, the results of the conceptual model need to be verified by a realistic ENSO model, and new findings on SPB are anticipated.

Mu *et al.* (2007b) used the intermediate-complexity model developed by Zebiak and Cane (1987; hereafter referred to as ZC) to investigate the SPB for El Niño events, but they did not pay attention to the effect of the different phases (the growth phase and the decaying phase) of El Niño or to the role of the intensity of El Niño events in the SPB. Furthermore, they did not identify which features display the initial error that causes a 'significant SPB' for El Niño events. Especially, they did not emphasize the role of nonlinearity despite the CNOP approach being used. In this paper, we attempt to address these questions by using the realistic ZC model.

The 'significant SPB' referred to here is the phenomenon that ENSO forecasting has a large prediction error; in particular, a prominent error growth occurs during the spring when the prediction is made before the spring. CNOP represents the initial error that induces the largest prediction error at the prediction time and has the potential for yielding a significant SPB (Mu *et al.*, 2007b). In this study, we therefore use the CNOP approach to address the above questions about the SPB.

The paper is organized as follows: the CNOP approach is introduced in section 2, and the CNOP-type errors superimposed on El Niño events are calculated and then compared with the LSV-type errors in section 3. In section 4, the SPB phenomenon of CNOP-type errors for El Niño events is explored. As a comparison, the evolution of the LSV-type errors is also investigated in section 4, while that of random initial errors is explored in section 5. Based on the results demonstrated in sections 3–5, we reveal some implications in section 6. Finally, the main results are summarized and discussed in section 7.

2. Conditional nonlinear optimal perturbation

The CNOP is an initial perturbation that satisfies a given constraint and has the largest nonlinear evolution at the prediction time (described below). The CNOP approach is a natural generalization of the LSV approach to a nonlinear regime. It has been used to study the nonlinear dynamics of ENSO predictability (Mu and Duan, 2003; Duan *et al.*, 2004; Duan and Mu, 2006; Mu *et al.*, 2007a, 2007b; Duan *et al.*, 2008), and the sensitivity of ocean circulation (Mu *et al.*, 2004; Sun *et al.*, 2005; Terwisscha van Scheltinga and Dijkstra, 2008; Wu and Mu, 2009). Recently, the CNOP approach has also been used to determine the 'sensitive area' in target observations for typhoons (Mu and Zhou, 2009). These studies have shown that CNOP is a useful tool for studying weather and climate predictability. For readers' convenience, we briefly review the CNOP approach as follows.

Let $M_{t_0,t}$ be the propagator (i.e. the numerical model) of a nonlinear model from initial time t_0 to t. u_0 is an initial perturbation superimposed on the basic state $U(t)$, which is a solution to the nonlinear model and satisfies $U(t) = M_t(U_0)$, with U_0 being the initial value of basic state $U(t)$.

For a chosen norm $||\cdot||$, an initial perturbation $u_{0\delta}$ is called CNOP if and only if

$$J(u_{0\delta}) = \max_{||u_0|| \leqslant \delta} \left\| M_{t_0,t}(U_0 + u_0) - M_{t_0,t}(U_0) \right\|, \quad (1)$$

DOI: 10.1002/qj

where $||u_0|| \leqslant \delta$ is the initial constraint defined by the chosen norm $||\cdot||$. The norm $||\cdot||$ also measures the evolution of the perturbations. Obviously, we can also investigate a situation in which the initial perturbations belong to another kind of functional set. Furthermore, the constraint condition could reflect some physical laws that the initial perturbation should satisfy.

CNOP is the initial perturbation whose nonlinear evolution attains the maximal value of the cost function J at time τ (Mu *et al.*, 2003; Mu and Zhang, 2006). In predictability studies, CNOP, rather than LSV, represents the initial error that has the worst effect on the prediction result at the optimization time (Mu *et al.*, 2003). CNOP has therefore been used to identify the initial error that causes the largest prediction error for ENSO events (Xu and Duan, 2008) and to determine the initial error that is most likely to cause a significant SPB of the El Niño events in a theoretical model (Mu *et al.*, 2007a). With the ZC model, the CNOP approach is also preliminarily applied to explore the initial error that exhibits season-dependent evolution related to the SPB for El Niño events (Mu *et al.*, 2007b). Based on these studies, in this paper we identify the common characteristics of the initial errors that cause a significant SPB for El Niño events and explore the respective effects of phases and intensities of El Niño events on the SPB, in an attempt to reveal the effect of nonlinearity by comparing CNOP with LSV.

To compute CNOP, one needs to solve Eq. (1). We notice that Eq. (1) is a maximization optimization problem and there is no solver to calculate it. However, there exist many solvers ready to deal with minimization optimization problems. Therefore, we have to transfer Eq. (1) into a minimization problem by considering the negative of the cost function. Then some solvers such as Spectral Projected Gradient 2 (SPG2: Birgin *et al.*, 2000), Sequential Quadratic Programming (SQP: Powell *et al.*, 1982), and Limited memory Broyden–Fletcher–Goldfarb–Shanno (L-BFGS: Liu and Nocedal, 1989) etc. can be used to compute CNOP. In these solvers, the gradient of the modified cost function is necessary; furthermore, the adjoint of the corresponding model is usually used to obtain the gradient. With this gradient information, running these solvers with initial guesses can find the minimum of the modified cost function (i.e. the maxima of the cost function in Eq. (1)) along the descendent direction of the gradient. In a phase space, the point corresponding to the minimum of the modified cost function is the CNOP defined by Eq. (1). In this paper, we use the SPG2 solvers to obtain the CNOPs of the ZC model. To obtain a CNOP, we try at least 30 initial guesses chosen randomly, in which, if there exist several initial guesses that converge to a point in the phase space, this point can be considered as a minimum in a neighbourhood. Thus, several such points are obtained. Of these points, the one that makes the cost function in Eq. (1) the largest is regarded as the CNOP.

3. CNOP-type errors of El Niño events in the ZC model

The ZC model is a nonlinear anomaly model of intermediate complexity that describes anomalies about a specified seasonally varying background, avoiding the 'climate drift' problem (Zebiak and Cane, 1987). The atmosphere model is a grid-point model with zonal resolution of $5.625^\circ \times 2.0^\circ$. The ocean model is run at a horizontal resolution of $2.0^\circ \times 0.5^\circ$. The ZC model has been routinely used in real time for ENSO forecasting since 1986. In particular, it is one of the few real-time models that predicted the onset of the 1991/1992 warm ENSO phase successfully. Its successful performance makes this model widely used in prediction and predictability studies. The model describes the essential physics of ENSO and can be regarded as a tool for investigating the SPB of ENSO.

As stated earlier, a significant SPB is considered here to consist in ENSO forecasting with a large prediction error, particularly a considerable growth in error through spring. CNOP represents the initial error that causes the largest prediction uncertainty and that may have potential for inducing the SPB phenomenon (Mu *et al.*, 2007b). Therefore, we first compute the CNOP-type errors superimposed on El Niño events that are produced by integrating the ZC model with an appropriate initial value.

We construct a cost function to measure the evolution of initial error. The aforementioned CNOP, denoted by $u_{0\delta}$, can be obtained by solving the following nonlinear optimization problem:

$$J(\vec{u}_{0\delta}) = \max_{||\vec{u}_0||_1 \leqslant \delta} ||\vec{T}'(\tau)||_2, \tag{2}$$

where $\vec{u}_0 = (w_1^{-1}\vec{T}'_0, w_2^{-1}\vec{h}'_0)$ is a non-dimensional initial error of the SSTA and thermocline depth anomaly superimposed on the initial state of a predetermined reference-state El Niño event. $w_1 = 2^\circ$C and $w_2 = 50$ m are the characteristic scales of SST and thermocline depth. $||\vec{u}_0||_1 \leqslant \delta$ is the constraint condition defined by a prescribed positive real number δ and the norm $||\vec{u}_0||_1 = \sqrt{\sum_{i,j}\{(w_1^{-1}T'_{0i,j})^2 + (w_2^{-1}h'_{0i,j})^2\}}$, where $T'_{0i,j}$ and $h'_{0i,j}$ represent the dimensional initial error of the SSTA and thermocline depth anomaly at different grid points and (i, j) is the grid point in the domain of the tropical Pacific with latitude and longitude, respectively, from 129.375°E to 84.375°W by 5.625° and from 19°S to 19°N by 2°. The evolution of the initial error is measured by $||\vec{T}'(\tau)||_2 = \sqrt{\sum_{i,j}(T'_{i,j}(\tau))^2}$. $\vec{T}'(\tau)$ represents the prediction error of SSTA at time τ and is obtained by subtracting the SSTA of the reference state from the predicted SSTA at prediction time τ.

Integrating the ZC model for 1000 years, we obtain a time series of SSTA, which provides a great number of El Niño events. These El Niño events tend to have a 4-year period and phase-lock to the end of the calendar year. In numerical experiments, we choose many El Niño events

DOI: 10.1002/qj

and find that results depend on the intensities of El Niño events. Therefore, in the context we use two groups of El Niño events to describe the results: one group consisting of weak events with Niño-3 indices (the SSTA averaged over the Niño-3 region) less than 2.5°C; the other group including strong events, with Niño-3 indices larger than 2.5°C. Considering that there exist different types of El Niño events in nature, we choose respectively in each group four events with initial warming times in January, April, July, and October, where the corresponding weak and strong events are denoted by WR_i and SR_i ($i = 1, 2, 3, 4$). Figure 1 shows the time-dependent Niño-3 indices for these two groups of El Niño events.

For each El Niño event, we make predictions for 12 months (i.e. leading time is 12 months) with different start-months. In the context, we use Year (0) to denote the year when El Niño attains a peak value, and Year (−1) and Year (1) to signify the year before and after Year (0), respectively. In numerical experiments, the El Niño predictions are first made with a start-month of July (−1) (i.e. July in Year (−1)), October (−1), January (0) (i.e. January in Year (0)), and April (0). These four predictions start in the season before the boreal spring and cross through the spring in the growth phase of El Niño. For convenience, we hereafter refer to these predictions as growth-phase predictions. Subsequently, we perform further numerical experiments for El Niño prediction with a start-month of July (0), October (0), January (1) (i.e. January in Year (1)), and April (1). Nevertheless, these four predictions are the ones passing through the spring in the decaying phase of El Niño and therefore referred to as decaying-phase predictions hereafter.

To investigate whether or not a significant SPB phenomenon occurs during each forecast, CNOP-type errors, i.e. the initial errors that have the largest effect on prediction uncertainties, are computed, where the initial times are the predetermined start-months of the El Niño forecasting and the time interval length is 12 months (i.e. $\tau = 12$ months, corresponding to a lead time of 12 months of El Niño prediction). The constraint bound δ (see section 2) related to CNOP is predetermined experimentally as 0.8, which represents a constraint bound and implies that the errors of SSTA and thermocline depth anomaly measured by the chosen norm do not exceed 0.8 (dimensional SSTA 1.6°C and thermocline depth anomaly 40 m), respectively. Consequently, a total of 64 CNOP-type errors are obtained. These resultant CNOP-type errors consist of two components of SSTA and thermocline depth anomaly. By investigating their patterns, we find that the SSTA components always have a localized region in the tropical Pacific, and the thermocline depth anomaly components tend to be positive (or negative) anomalies along the Equator despite there existing numerical grid noise in their patterns. This grid noise may result from computational instability, which could cause some uncertainties in the pattern structure of thermocline depth anomalies of CNOP-type errors. To offset such uncertainties as far as possible, taking the ensemble mean may be an acceptable approach. We first perform a cluster analysis for the 64 CNOP-type errors, with the similarity coefficient as the measurement, and

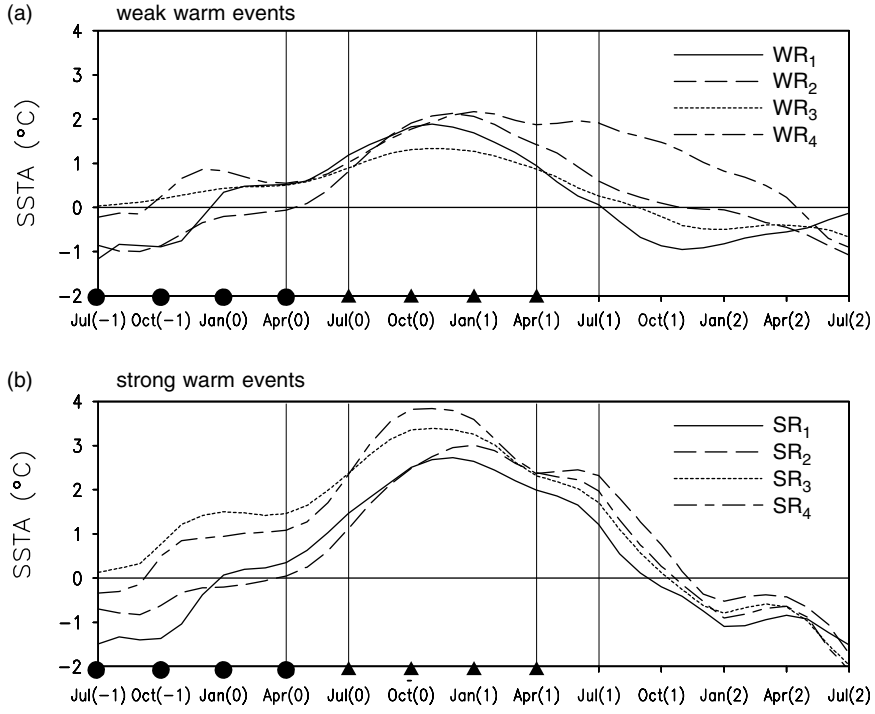

Figure 1. Reference-state El Niño events. (a) The time-dependent Niño-3 indices of four weak El Niño events, denoted by WR_i, $i = 1, 2, 3$ and 4; and (b) those of four strong El Niño events, signified by SR_i, $i = 1, 2, 3$ and 4. The start-months of predictions for these El Niño events are marked on the horizontal axis, where July(−1), October(−1), January(0), and April(0) are the start-months of the growth-phase predictions, while July(0), October(0), January(1), and April(1) are those of the decaying-phase predictions.

DOI: 10.1002/qj

classify them into two groups, with 36 in one and 28 in the other, and then take respectively the ensemble mean of the SSTA and thermocline depth anomaly components of CNOP-type errors in each group. Consequently, two pairs of smoother composite patterns of the SSTA and thermocline depth anomaly are obtained (Figure 2). It is illustrated that the composite thermocline depth anomaly component undergoes deepening along the Equator in one group, and the corresponding SSTA pattern has a structure with negative anomalies in the equatorial central-western Pacific and positive anomalies in the equatorial eastern Pacific while those in the other group have signs almost opposite to the former. These indicate that the CNOP-type errors related to these predictions can be classified into two types. We refer to these two kinds of CNOP-type errors as type-1 and type-2 CNOP errors, respectively. In addition, we also notice that the CNOP-type errors associated with the growth-phase predictions of the strong El Niño events are mostly the type-2 CNOP errors, while most of those correlated with the decaying-phase predictions are the type-1 CNOP errors. However, for the weak El Niño events, it is very difficult to determine which type of CNOP error is dominant in the growth-phase and decaying-phase predictions, respectively.

To compare the above CNOP-type errors with their linear counterparts, we also investigate the corresponding LSV-type errors of the given El Niño events in Figure 1, where the LSV-type errors are computed by replacing the nonlinear model in Eq. (2) with its linearized version. The results demonstrate that the LSV-type errors with the same magnitude as CNOP-type errors have a large-scale zonal structure similar to those of the CNOP-type errors and, consequently, can also be classified into two types, but they possess a more localized spatial region than the CNOP-type errors. Furthermore, for a prediction with a lead time and a given magnitude of initial errors, the two types of LSV error, i.e. an LSV named as type-1 LSV error and its negative pattern −LSV named as type-2 LSV error, are obtained simultaneously and fully symmetric. That is to say, if initial error u_{0L} is a type-1 LSV error of an El Niño prediction, its negative pattern $-u_{0L}$, known as a type-2 LSV error, is also an LSV-type error of this prediction. However, for the CNOP-type error of an El Niño prediction, we cannot regard its negative as a CNOP-type error of this prediction. In other words, although the type-1 and type-2 CNOP errors are almost the negative of each other (but not fully symmetric), they represent the optimal initial errors of different El Niño predictions. The difference between CNOP and LSV reflects the effect of nonlinearity and indicates that LSV could not be the initial error that has the largest effect on prediction in the nonlinear ZC model. Due to this limitation of the singular vector, we would rather believe that CNOP-type error with an eye to nonlinearity captures such optimal initial error and is therefore more applicable in exploring the significant SPB.

From the above results, it is clear that the initial errors that have the largest effect on prediction are identified as two types of CNOP-type error in prediction experiments of model El Niño events, giving rise to new questions. How does seasonality related to SPB affect the growth of these CNOP-type errors? What is the difference

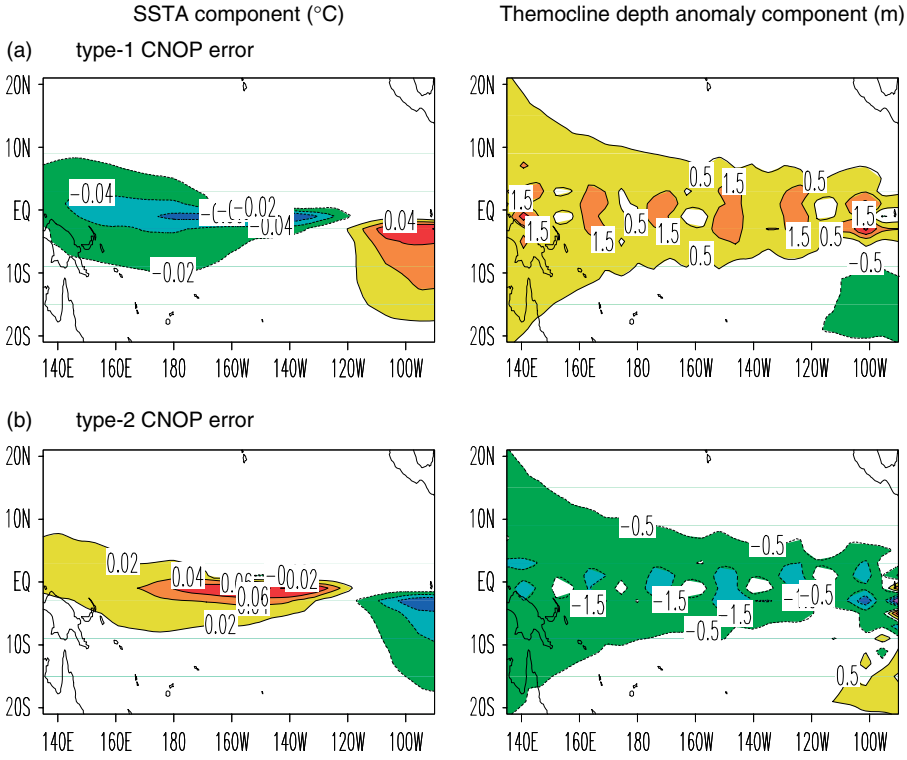

Figure 2. The patterns of two categories of 64 CNOP-type errors. The left column is for the SSTA component, and the right column is for the thermocline depth anomaly. The pattern in (a) is the type-1 CNOP error; and that in (b) the type-2 CNOP error. This figure is available in colour online at www.interscience.wiley.com/journal/qj

DOI: 10.1002/qj

between the prediction uncertainties caused by the two types of CNOP-type error for the corresponding El Niño events? Is there any difference in the SPB phenomenon between the growth-phase prediction and the decaying-phase prediction? What is the role of nonlinearity in SPB? In the following, we will address these questions by tracing the evolution of CNOP-type errors.

4. The SPB phenomenon for the El Niño events in the ZC model

As mentioned in the introduction, a significant SPB here is related to the phenomenon that ENSO forecasting has a large prediction error; in particular, a prominent error growth occurs during the spring when the prediction is made before the spring. The CNOP-type error causes the largest prediction error and may be the initial error that is most likely to induce a significant SPB. In the following, we will address the SPB problem from two aspects: (1) the prediction errors caused by the CNOP-type errors and (2) season-dependent evolution of the CNOP-type errors.

To study the seasonal dependence of CNOP-type error evolution, we divide a calendar year into four seasons starting with January to March (JFM), followed by April to June (AMJ), and so forth. The slope of the curve $\gamma(t) = ||T'(t)||_2$ at different seasons is then evaluated, where $T'(t)$ is the same as in section 3 and represents the SSTA component of the nonlinear evolution of CNOP-type error. The slope of $\gamma(t)$, denoted by κ, indicates the growth tendency of CNOP-type error at different seasons. A positive (negative) value of κ implies an increase (decrease) of the error, and the larger the absolute value of κ, the faster the increase (decrease) of the error.

It has been mentioned that, for each reference-state El Niño event, the predictions with a start-month of July (−1), October (−1), January (0), and April (0) and a lead time of 12 months cross the boreal spring (AMJ) in the growth phase of the El Niño event, while those with a start-month of July (0), October (0), January (1), and April (1) pass through the spring in the decaying phase of the El Niño event. To investigate the SPB phenomenon in these predictions, we estimate the seasonal growth rates (as measured by the slope κ) of the CNOP-type errors shown in section 3. We show that the CNOP-type errors, whichever phase of El Niño events they correspond to, always exhibit significant season-dependent evolution and cause the largest prediction uncertainties, yielding a significant SPB. In particular, the predictions made through the spring in the growth phase of El Niño with a lead time of 12 months have much larger uncertainties than those made across the spring in the decaying phase. Furthermore, when forecasting starts directly in the spring, the prediction uncertainties are much smaller than those of predictions starting in other seasons. For the LSV-type errors, they usually cause a smaller prediction error than the corresponding CNOP-types and induce a relatively weak SPB phenomenon. To illuminate these results and gain insight into the influence of nonlinearity on season-dependent predictability, we describe the details of the strong and weak El Niño events shown in section 3.

4.1. Cases of the growth-phase predictions for El Niño

As described in section 3, predictions starting from July (−1), October (−1), January (0) and April (0) straddling the boreal spring (AMJ) in the growth phase of El Niño events are called growth-phase predictions. With these start-months, we predict the El Niño event by integrating the ZC model with an initial condition of the value of the El Niño event at the start-month plus the corresponding CNOP-type error. Then, the evolution of CNOP-type error, $\gamma(t)$, is obtained by removing the reference-state El Niño from the predicted one. In doing so, the error growth rate measured by the slope κ can be evaluated. It is demonstrated that the El Niño events with different initial warming times show similar results. Therefore, we illustrate the seasonal growth tendency of the CNOP-type error by using the ensemble mean of the slopes κ for weak and strong El Niño events, respectively.

In Figure 3(a), we plot the histogram for the ensemble mean of the slopes κ with a prediction start-month of July (−1) for weak and strong El Niño events, respectively. It is illustrated that the CNOP-type errors, either for the strong El Niño events or weak El Niño events, tend to have their largest growth rate in the AMJ season and exhibit significant season-dependent evolution. Considering that a significant SPB here consists of both prominent season-dependent evolution and large prediction error, we also plot in Figure 4(a) the prediction errors caused by the CNOP-type errors, where $E_{\text{Niño}-3}$ represents the uncertainty caused by the CNOP-type error of the El Niño prediction with one-year lead time, a value which is obtained by subtracting the Niño-3 index of the reference state from the predicted one. A positive (negative) value of $E_{\text{Niño}-3}$ shows a positive (negative) prediction error in NINO-3 SSTA and indicates an overprediction (underprediction) of the event. The values of $E_{\text{Niño}-3}$ shown in Figure 4(a) demonstrate that the CNOP-type errors associated with some of the eight El Niño events cause a positive error of NINO-3 SSTA and induce an overprediction of the corresponding El Niño events, while those of other El Niño events lead to a negative error in NINO-3 SSTA and an underprediction of the El Niño events. Furthermore, we find that most of the CNOP-type errors that cause an overprediction of events resemble the type-1 CNOP error shown in Figure 2, while those errors that cause an underprediction of the events resemble the type-2 CNOP error. In any case, these two CNOP-type errors cause not only the largest prediction uncertainties but also a prominent season-dependent evolution and can therefore be regarded as most likely to cause a significant SPB for El Niño.

For the El Niño predictions starting from October (−1) and January (0), we also investigate the season-dependent evolution of the corresponding CNOP-type errors (see Figure 3(b) and (c)). The results illustrate that the CNOP-type errors of some El Niño events tend to

DOI: 10.1002/qj

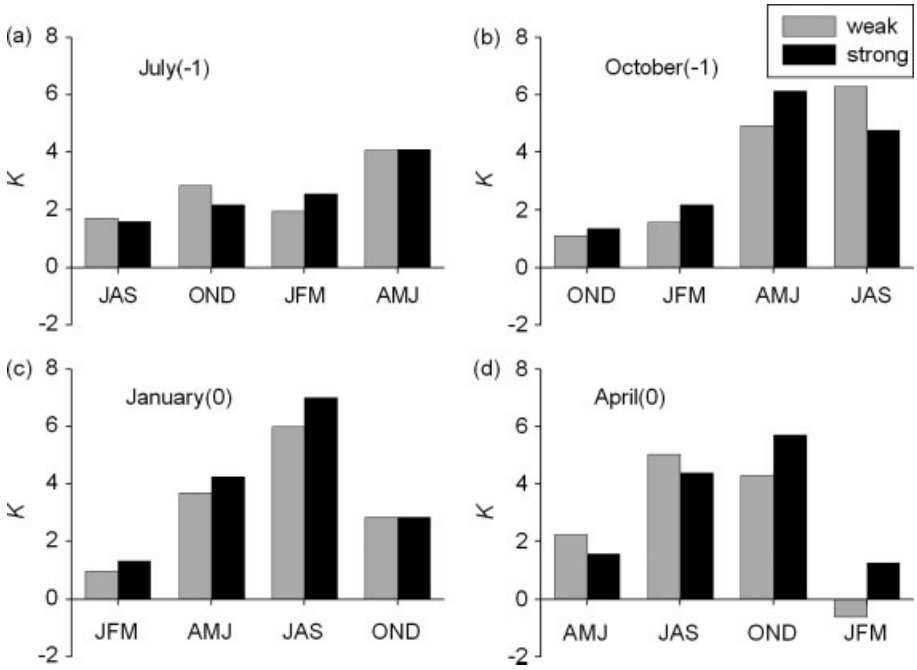

Figure 3. Ensemble mean of seasonal growth rate κ of CNOP-type errors for the weak and strong El Niño events shown in Figure 1, respectively. The start-months of predictions are (a) July(−1), (b) October(−1), (c) January(0) and (d) April(0). For the predictions made before the boreal spring, the largest growth of the CNOP-type errors tends to be in the AMJ or JAS seasons. Although sometimes the largest growth appears in the JAS season, the error growth during AMJ has become aggressively large and may have also caused the drastic decrease in El Niño forecast skill across the spring, yielding the SPB.

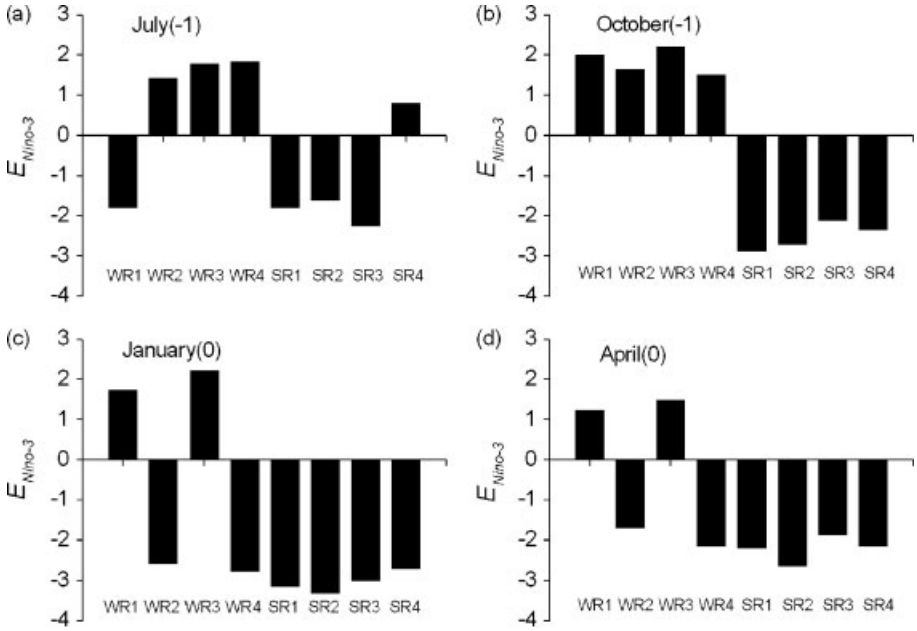

Figure 4. Prediction errors of the eight El Niño events shown in Figure 1, which are caused by their respective CNOP-type error with start-months of (a) July(−1), (b) October(−1), (c) January(0) and (d) April(0).

grow significantly in AMJ, while those of other El Niño events have considerable growth in both AMJ and July to September (JAS), with the largest growth rate in JAS. For El Niño predictions with a start-month in January (0), the largest growth rates of the CNOP-type errors for the eight El Niño events are always in JAS. For this situation, Mu *et al.* (2007b) argued that although the largest growth of the initial errors occurs in the JAS season, the error growth during AMJ has become aggressively large and may have caused the drastic decrease in El Niño forecast skill across the spring. Despite this difference, the CNOP-type errors with a start-month of October (−1) or January (0) can still be classified into two types based on the signs of their resultant prediction errors (see Figure 4(b) and (c)). The first consists of the errors that cause overprediction of the corresponding El Niño event and that possess an SSTA pattern with negative anomalies in the equatorial central-western Pacific, positive anomalies

DOI: 10.1002/qj

in the equatorial eastern Pacific, and a thermocline depth anomaly pattern with a deepening tendency along the Equator (i.e. the type-1 CNOP error shown in section 3); the other type includes the errors that cause underprediction of the El Niño event, with SSTA and thermocline depth anomaly patterns almost opposite to those of the type-1 CNOP (i.e. the type-2 CNOP shown in section 3).

The above growth-phase predictions with three start-months have demonstrated that the CNOP-type errors are classified into two types of patterns; furthermore, they cause a prominent season-dependent evolution and the largest prediction error of the corresponding El Niño event, yielding a significant SPB. In particular, we notice that, for the strong El Niño events, the errors of the growth-phase predictions caused by their respective CNOP-type errors are almost always negative (see Figure 4(a), (b) and (c)); however, for the weak El Niño events, the resultant prediction errors are either positive or negative. This observation indicates that, when predictions are made starting from the pre-spring season in the growth phase of El Niño events, the initial errors with the largest effect on the prediction of the strong El Niño events could always be the type-2 CNOP errors. That is to say, for the strong El Niño events, the initial error that is most likely to cause a significant SPB in the growth-phase prediction tends to be the type-2 CNOP error, a conclusion that coincides with the results shown in section 3.

We further explore the growth-phase predictions of El Niño with a start-month of April (0) (see Figure 3(d)). The month April (0) is the beginning of the AMJ season, meaning that these predictions start directly in the spring. The results obtained demonstrate that, for the two groups of reference-state El Niño events, the CNOP-type errors with an initial time of April (0) can also be classified into two types of pattern similar to those of the type-1 and type-2 CNOP errors. Nevertheless, we notice that although the predictions for the strong El Niño events also show that the initial errors with the largest effect tend to be type-2 CNOP errors, any significant growth of the initial errors, for either strong or weak El Niño events, mostly occurs in either the JAS or October–November–December (OND) seasons. That is, when the growth-phase predictions are made directly in the spring, the decrease of the forecast skill for the El Niño event during either the JAS or the OND season is the most dramatic, while the decrease seen during the spring (AMJ) is not nearly as significant. Furthermore, these predictions are much easier than those starting from other seasons (the details are seen in Figure 6 in the next section) though they also have considerable prediction uncertainties (see Figure 4(d)).

Now we discuss the superiority of CNOP in revealing a significant SPB. As demonstrated in section 3, there exists only one CNOP of an El Niño prediction, which resembles either the type-1 CNOP error or the type-2 CNOP error. Furthermore, this section has shown that the CNOP-type error in each prediction causes a prominent season-dependent evolution and the largest prediction error for the corresponding El Niño event, being most likely to yield a significant SPB. However, for the LSV-type error, we have to explore simultaneously two fully symmetric patterns, type-1 (LSV) and type-2 (−LSV) LSV errors, due to its linearity (see section 3; Figure 5), and compare them with the corresponding CNOP-type error. The results demonstrate that, although both these two kinds of LSV-type error also exhibit a season-dependent evolution (see Figure 5), they cause much smaller prediction errors than the CNOP-type errors do (Figure 6), consequently inducing a much weaker SPB.

From the above results, we see that when the El Niño events are predicted through the spring in the growth phase, the CNOP-type errors tend to exhibit an apparent season-dependent growth and cause the largest prediction uncertainties, therefore yielding a significant SPB phenomenon. These CNOP-type errors are classified into two types that have clear spatial characteristics. Furthermore, the CNOP-type errors associated with the growth-phase predictions for strong El Niño events closely resemble the type-2 CNOP errors. Although the LSV-type errors also cause an SPB, it is less significant than that caused by the corresponding CNOP-type errors, implying that the nonlinearities increase the uncertainties of the growth-phase predictions for El Niño events through the spring. The subsequent question is whether the above properties of the CNOP-type errors related to the significant SPB can be shown in the decaying-phase predictions for the two groups of reference-state El Niño events.

4.2. Cases of decaying-phase predictions for El Niño

In the eight predictions for each El Niño event, the ones with start-month July (0), October (0), January (1) and April (1) cross the spring in the decaying phase of the El Niño events. As before, we investigate the seasonal growth rate of the CNOP-type errors related to these decaying-phase predictions. For the eight chosen El Niño events, the CNOP-type errors have been obtained in section 3. As for the slopes κ related to these CNOP-type errors, we show that, for predictions with a start-month of July (0), October (0), or January (1), the corresponding CNOP-type errors exhibit significant season-dependent evolution and cause the largest prediction error, yielding a significant SPB. Also, all the CNOP-type errors can be classified into two types based on the signs of their resultant prediction errors: one type causes a positive error and has a pattern similar to that of the type-1 CNOP errors, while the other type causes a negative prediction error and has a similar pattern to the type-2 CNOP errors. For the LSV-type errors, they usually cause a much smaller prediction error than the corresponding CNOP-type errors do, then yielding a weaker SPB phenomenon. These results coincide with those found for the growth-phase predictions of the El Niño events. The details are therefore omitted.

Differences do exist between the results of the growth-phase and decaying-phase predictions. One discrepancy lies in the types of CNOP-type error seen in the growth-phase prediction for the strong El Niño events as opposed

DOI: 10.1002/qj

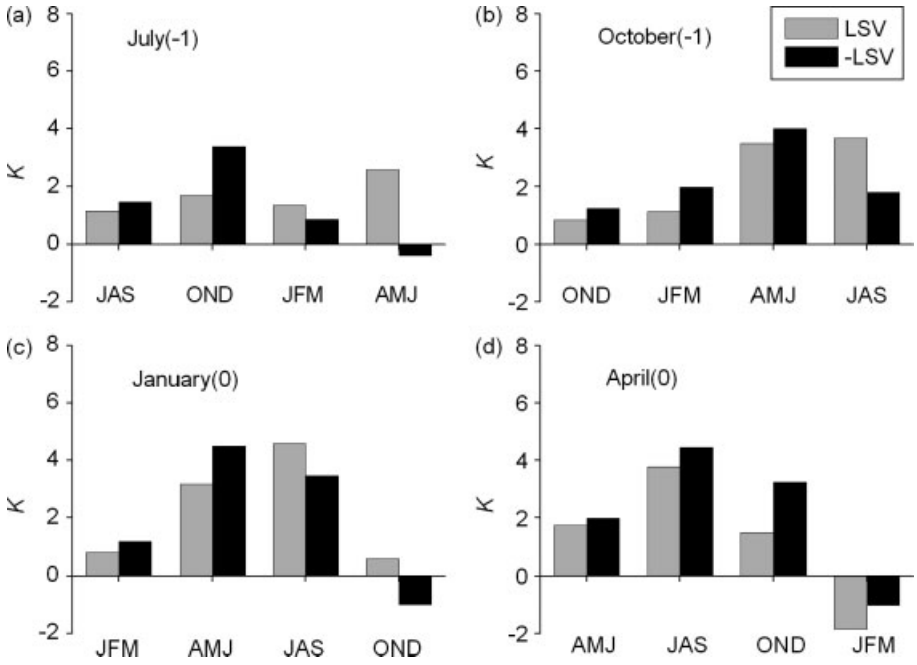

Figure 5. Ensemble mean of seasonal growth rate κ of two kinds of LSV error (LSV and −LSV) for the eight El Niño events. The start-months of predictions are (a) July(−1), (b) October(−1), (c) January(0) and (d) April(0).

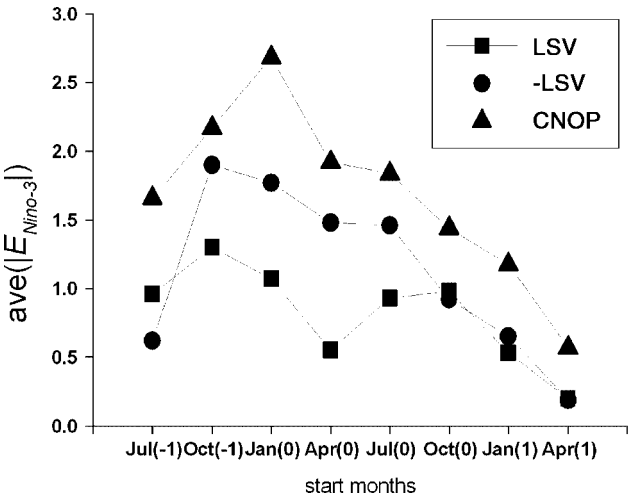

Figure 6. Averaged prediction errors for the eight El Niño events with each start-month and a lead time of 12 months, which is measured by the absolute value of $E_{\text{Niño}-3}$. Here are plotted the prediction errors caused by the corresponding CNOP-type errors and two LSV-type errors with opposite signs (LSV and −LSV), respectively.

to those of the decaying-phase. We have shown that most of the CNOP-type errors related to the growth-phase prediction barrier for the strong El Niño events are close to the type-2 CNOP error, while those related to the decaying-phase prediction barrier usually resemble the type-1 CNOP error. This distinction indicates that the initial errors that are most likely to cause a significant SPB in the growth-phase predictions of strong El Niño events are different from those in the decaying-phase predictions; the former features type-2 CNOP error, while the latter is characterized by type-1 CNOP error. However, the LSV-type errors, whatever predictions they are related to, always show simultaneously two fully symmetric patterns of opposite signs, due to the linearity of singular vectors.

Another difference consists of the amplitude of prediction uncertainties between the growth-phase predictions and the decaying-phase predictions. In Figure 6, we show the averaged prediction errors of Niño-3 indices (denoted by 'ave($|E_{\text{Niño}-3}|$)') for the eight El Niño events with a one-year lead time. The start-months Jul(−1), Oct(−1), Jan(0), and Apr(0) correspond to growth-phase predictions; while the months Jul(0), Oct(0), Jan(1), and Apr(1) are associated with decaying-phase predictions. It is shown that the CNOP-type errors associated with growth-phase predictions for El Niño usually cause a larger prediction error than those associated with decaying-phase predictions. Furthermore, with a start-month from the season before the boreal spring to the spring, the prediction error associated with the growth-phase prediction becomes gradually larger, while that associated with the decaying-phase prediction gets increasingly smaller. Nevertheless, we note that the prediction starting directly from the spring in the growth phase of El Niño events does not have much larger uncertainties (in terms of the CNOP-type errors) than those predictions starting from other seasons in the growth phase. Despite this outcome, the prediction error caused by the CNOP-type errors with the start-month in the spring in the growth phase is considerably larger than that in the decaying phase. These results imply that predicting El Niño through the spring in the growth phase could be more difficult than doing so in the decaying phase, which coincides with the results of Karspeck *et al.* (2006). In addition, when the prediction starts directly in the spring, the prediction error caused by the CNOP-type errors is much smaller than that of predictions starting from other seasons. However, it is noticed that these results cannot be exactly obtained by the LSV

DOI: 10.1002/qj

approach. Since the CNOP-type approach considers the effect of nonlinearity, we would rather think that the results obtained by the CNOP approach are reasonable. Furthermore, we can identify the effect of nonlinearity from the difference between CNOP and LSV. In fact, from Figure 6 we show that the differences between the prediction errors caused by the CNOP-type errors and those by the LSV-type errors in the growth-phase predictions are larger than those in the decaying-phase predictions, which, actually, implies that the growth-phase predictions could be affected by a relatively strong nonlinearity compared to the decaying-phase predictions.

To sum up, in either the growth-phase prediction or the decaying-phase prediction, the CNOP-type errors cause the largest prediction error and exhibit a significant season-dependent evolution, and then yield a significant SPB phenomenon, while the LSV-type errors cause a smaller prediction error and show a less significant SPB phenomenon. This indicates that the nonlinearity increases the uncertainties of the El Niño predictions through the spring. In particular, the effect of nonlinearity on the growth-phase predictions could be larger than that on the decaying-phase predictions. In addition, it is noted that different initial errors, such as the CNOP-type errors and the LSV-type errors, exhibit different amplitude of SPB, which implies that the SPB could be closely related to the patterns of initial error. Then the remaining questions are whether there are other kinds of initial errors with the same magnitudes as the CNOP-type errors and the LSV-type errors in terms of the chosen norm, which either have a trivial effect on the prediction results or experience negligible growth during the spring in either the growth phase or the decaying phase and do not yield the SPB.

5. Behaviour of random initial errors on El Niño events

Mu *et al.* (2007b) has illustrated that there exist some initial errors that cause trivial prediction uncertainties and lack readily apparent season-dependent evolution. However, such initial errors in Mu *et al.* (2007b) were yielded with a deterministic approach. In some ENSO prediction studies, random initial errors were also superimposed on El Niño events to explore ENSO's predictability. In this section, we explore whether or not random initial errors with the same magnitude as CNOP-type errors also yield an SPB phenomenon similar to that caused by the CNOP-type errors.

For each start-month of the prediction of each El Niño event, several random initial errors are generated whose components consist of the SSTA and the thermocline depth anomaly just as those of the CNOP-type errors. The errors at each grid point satisfy a normal distribution. We scale these random initial errors with $\sigma \frac{u_R}{||u_R||_1}$, where σ is a positive real number and u_R denotes a random initial error. For each u_R, we make $\sigma = 0.8$ and then obtain a scaled random initial error $u_{R_0} = \sigma \frac{u_R}{||u_R||_1}$ with the magnitude being $||u_{R_0}||_1 = 0.8$.

The two groups of El Niño events in Figure 1 are predicted for a one-year lead time by integrating the ZC model with initial conditions of the reference-state El Niño event at the start-month of predictions plus the random initial errors. By investigating the seasonal growth rates (measured by the slope κ) of these random initial errors, it is found that for both the growth-phase and the decaying-phase predictions of El Niño events, the random initial errors neither yield large prediction uncertainties nor exhibit any obvious season-dependent evolution and therefore do not cause the SPB phenomenon. Furthermore, the slope κ in each season is fairly small, meaning that the random initial errors have, at most, trivial growth in each season. To illustrate, we present the ensemble mean of slopes κ of the predictions for eight El Niño events with a start-month of July (-1) in Figure 7(a) and prediction errors of each El Niño event in Figure 7(b).

While random initial errors clearly do not cause the SPB phenomenon for El Niño events, the CNOP-type errors do cause a significant SPB and the LSV-type errors yield a less significant SPB. We infer that the occurrence of the SPB is related to the initial error patterns, though the seasonality originates from the annual cycle. This indicates that the SPB may be a result of the combined effects of the annual cycle, El Niño events, and particular initial errors, in which the positive feedback mechanism of Bjerknes (1969) could account for the growth of the initial errors related to the SPB.

6. Implications

The above results demonstrate that CNOP-type errors for the different types of El Niño event can be classified into type-1 and type-2 CNOP errors. When the prediction is made before and through the spring in the growth (decaying) phase of the El Niño event, the initial errors with the largest effect on the predictions tend to be the type-2 (type-1) CNOP errors. Furthermore, the growth-phase prediction uncertainties caused by the type-2 CNOP errors can be more severe than the decaying-phase prediction uncertainties caused by the type-1 CNOP errors. Then, in different phases of the El Niño events, there exist different amplitudes of the SPB phenomenon, with the ones related to the growth-phase predictions being more severe than the ones related to the decaying-phase prediction. Also, different patterns of initial errors cause different amplitudes of the SPB, which implies that the accuracy of the initial field is very important in reducing the El Niño prediction barrier. In fact, Chen *et al.* (1995; 2004) weakened the SPB phenomenon in the ZC model by improving the initialization procedure. Our results provide a theoretical explanation for this fact.

The presence of two types of CNOP-type errors suggests two kinds of dynamical behaviour in error growth related to the SPB. Type-1 CNOP errors yield a positive prediction error of the NINO-3 SSTA and cause an overprediction of the SSTA of the El Niño event, indicating that the type-1 CNOP errors have

DOI: 10.1002/qj

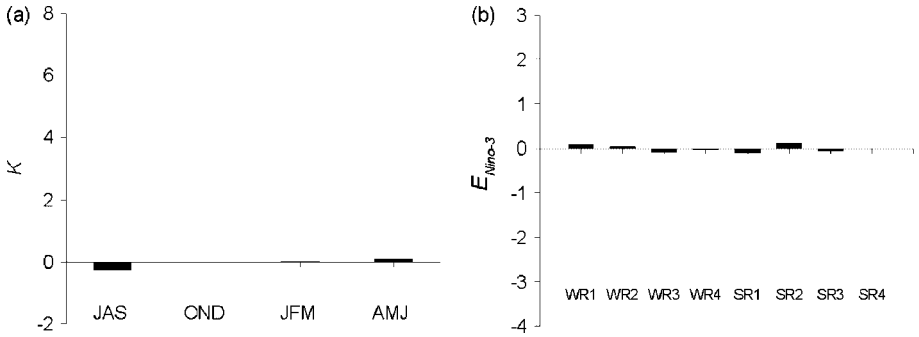

Figure 7. Behaviour of random initial errors. (a) The ensemble mean of seasonal growth rate κ of the random initial errors for eight El Niño events in Figure 1, with the start-month of prediction July (-1); (b) the prediction errors of the eight El Niño events caused by the random initial errors.

their effect by increasing the magnitude of the SSTA. We therefore infer that the type-1 CNOP errors could evolve into a positive SSTA, i.e. an El Niño-like event, since their growth behaviour is similar to that of an El Niño event. The type-2 errors have a sign almost opposite to that of the type-1 CNOP errors and may evolve into a negative NINO-3 SSTA, decreasing the NINO-3 SSTA and causing an underprediction of the NINO-3 SSTA for El Niño events. This implies that the type-2 CNOP errors have a growth tendency opposite to that of El Niño events. In order to verify these conclusions, we have examined the evolution of the two pairs of composite CNOP-type errors shown in Figure 2 by adding them in the different start-months of each El Niño event. In Figures 8 and 9, we plot the composite SSTA component of the evolutions of two composite CNOP-type errors associated with the growth-phase predictions and decaying-phase predictions for the strong El Niño events, respectively. The error growth related to the SPB may therefore have two different dynamical behaviours similar to those of the El Niño and La Niña events. Furthermore, El Niño and La Niña events are now understood to be the result of Bjerknes' (1969) positive feedback; meanwhile, they usually exhibit the fastest growth during spring, due to the springtime strongest ocean–atmospheric instability of the climatological annual cycle (Wang and Fang, 1996). These results then indicate that the error growth related to a significant SPB has the same growth mechanism as that of ENSO events, also resulting, in essence, from the Bjerknes positive feedback mechanism. In addition, although the two composite CNOP-type errors are almost the negative of each other, the growth-phase prediction errors caused by them, especially for the strong El Niño events, are considerably different in amplitude (Figure 8), while the decaying-phase prediction errors yielded by them are trivially different (Figure 9). All these imply that the growth-phase prediction, especially for the strong El Niño event, may be affected by relatively strong nonlinearities while the decaying-phase prediction is influenced by weak ones, a conclusion that can also be drawn by comparing the CNOP and LSV (see Figure 6).

Kirtman *et al.* (2002) demonstrated that the ENSO predictions starting directly from the spring are relatively easier than those starting from other seasons. In fact, our results confirm this argument. In particular, for predictions starting from the spring in the decaying phase, the CNOP-type errors cause smaller prediction errors than are produced for predictions with a start-month in the spring in the growth phase of El Niño events. This suggests that the SPB may result not because predictions made directly in the spring are relatively difficult compared to those made in other seasons and through the spring, but because there exists an apparent drop in prediction skill during the spring when the prediction is made before and runs through the boreal spring season.

In addition, we note that both types of CNOP error are associated with a localized region. The largest SSTA errors in all the CNOP-type errors are mainly localized in the equatorial central-east Pacific, a phenomenon that may reveal a 'sensitive area' of El Niño predictions. Intensifying observations in the sensitive area may greatly improve ENSO predictions. Although the LSV-type errors also have a localized region, they cover a much smaller area than the CNOP-type errors. That is to say, for the same magnitude of the CNOP- and LSV-type errors, the sensitive area determined by the former is broader than that by the latter. Then the El Niño prediction could be more significantly improved by intensifying observation in the sensitive area determined by the CNOP than in that obtained by the LSV. CNOP may be more useful than LSV in determining the sensitive area of El Niño prediction. Furthermore, we note that the type-1 CNOP errors cause an overprediction of El Niño events, while the type-2 CNOP errors cause an underprediction. This suggests that if multiple perturbed initial conditions are adopted to predict the El Niño events, the ensemble mean may offer a better forecast than a single forecast, in which case the CNOP patterns could also be useful for generating ensemble initial perturbation fields.

7. Conclusions and discussion

The 'spring predictability barrier' (SPB) problem in El Niño prediction is explored within the ZC model through the use of conditional nonlinear optimal perturbation (CNOP). The results show that the CNOP-type errors

DOI: 10.1002/qj

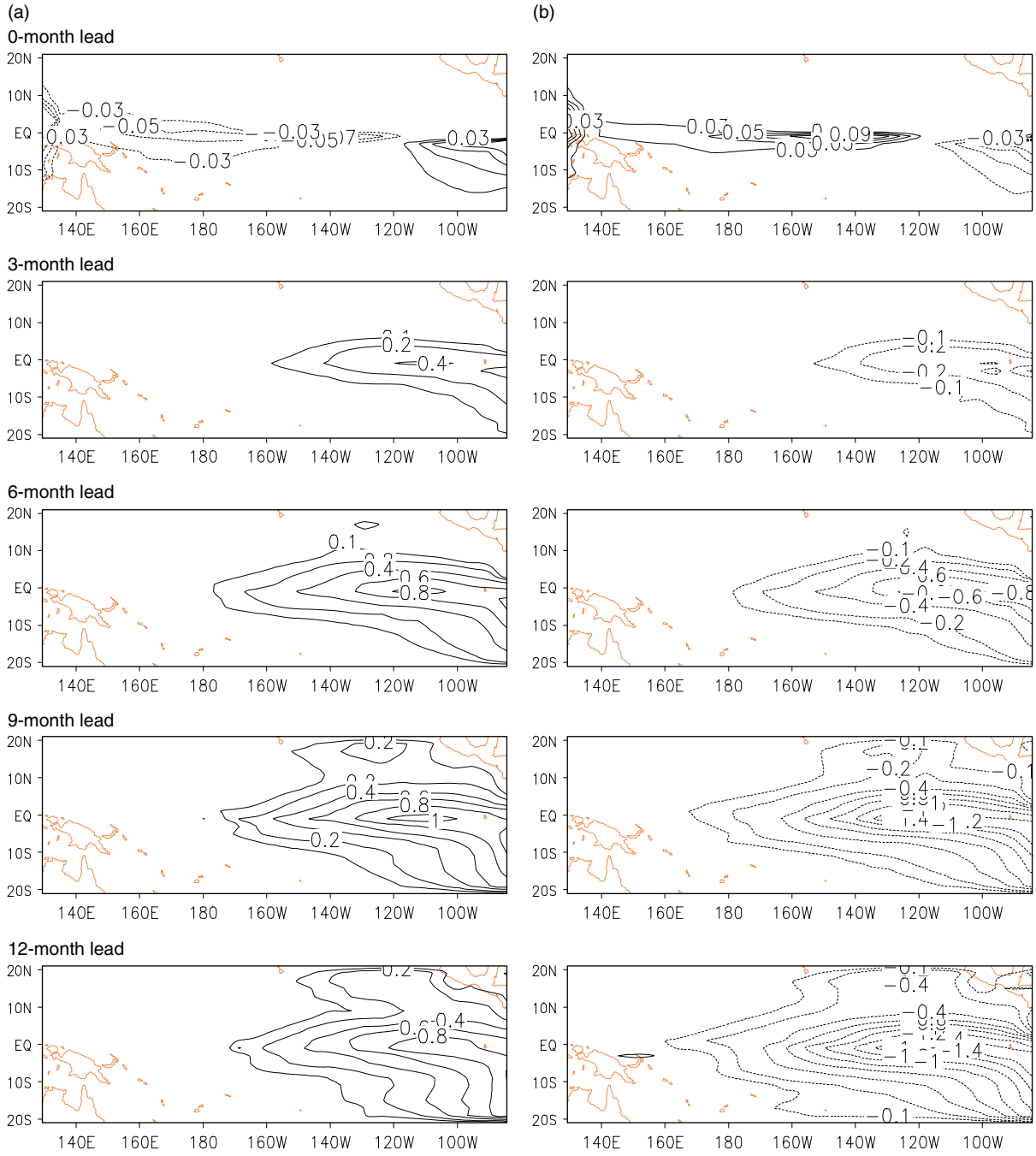

Figure 8. Composite of the SSTA component of the evolutions of the composite type-1 and type-2 CNOP errors, where the two types of CNOP error are respectively added in the different start-months of the growth-phase predictions for the strong El Niño events. (a) The evolution of the type-1 CNOP error, and (b) that of the type-2 CNOP error. This figure is available in colour online at www.interscience.wiley.com/journal/qj

of El Niño events can be classified into two types: the type-1 and the type-2 CNOP errors. The type-1 CNOP errors have an SSTA pattern with negative anomalies in the equatorial central-western Pacific, positive anomalies in the equatorial east Pacific, and a thermocline depth anomaly pattern with positive anomalies along the Equator, while the type-2 CNOP errors possess almost the opposite patterns. When a prediction is made starting before and crossing through the spring in the growth phase of strong El Niño events, the type-2 CNOP errors tend to be the initial errors with the worst effect on the growth-phase prediction; when the prediction is made through the spring in the decaying phase of strong El Niño events, the optimal initial errors are the type-1 CNOP errors. For weak El Niño events, it is very difficult to identify which type of CNOP error play the dominant role in the different phase predictions of El Niño events. In addition, we also demonstrate that the growth-phase prediction uncertainties caused by the CNOP-type errors are larger than the corresponding uncertainties for the decaying-phase prediction. Meanwhile, El Niño predictions with a start-month in the spring are relatively easier than those with a start-month in other seasons. This theoretical result supports those

DOI: 10.1002/qj

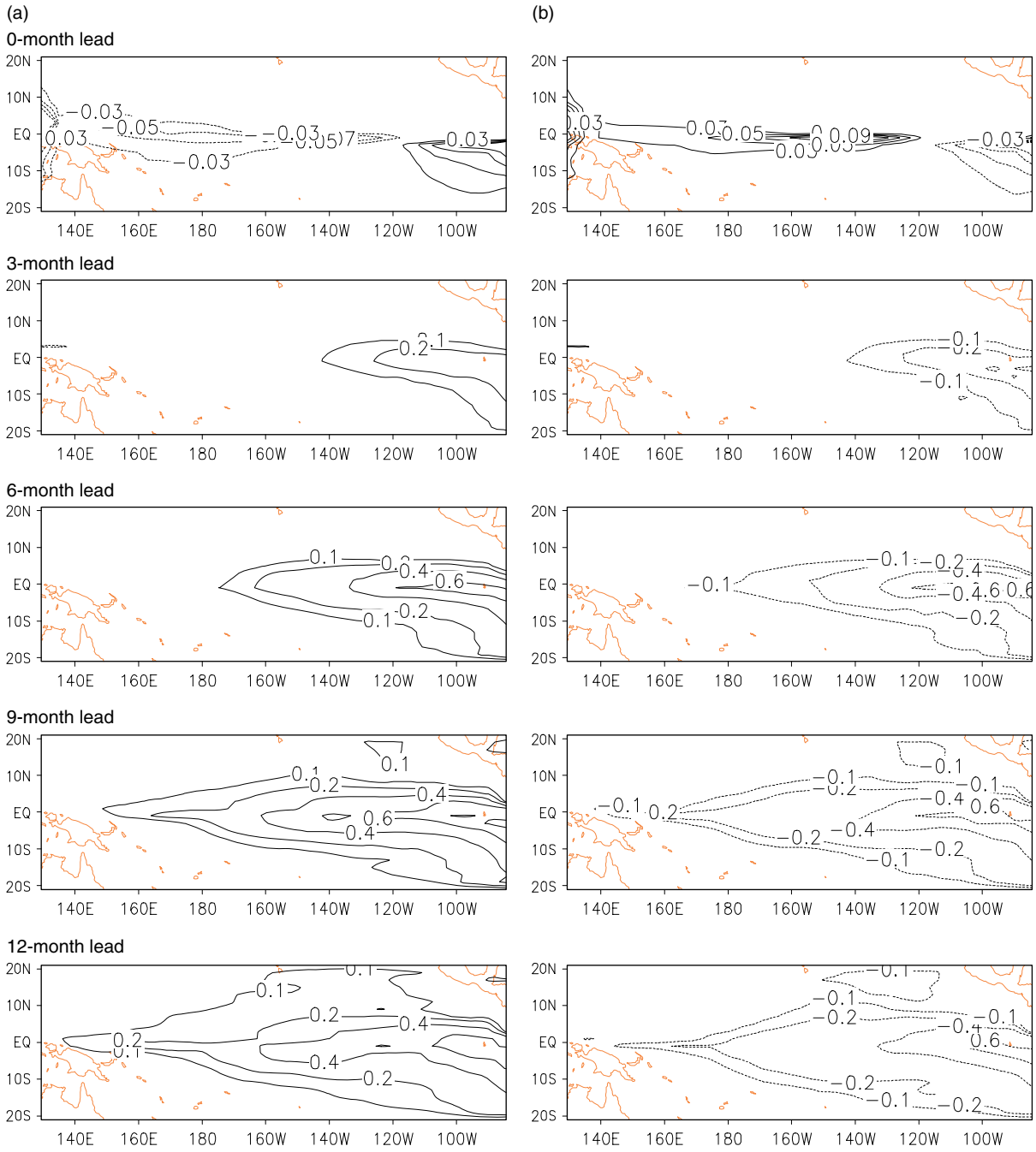

Figure 9. As in Figure 8, but for the decaying-phase predictions. This figure is available in colour online at www.interscience.wiley.com/journal/qj

of the ENSO hindcast experiments obtained by Kirtman *et al.* (2002).

Although the LSV-type errors possess patterns similar to the CNOP-type errors, they have a more localized spatial region and cause a smaller prediction error, yielding a weaker SPB for El Niño events. We also show that random initial errors neither cause a large prediction error nor exhibit a season-dependent evolution and therefore do not yield the SPB phenomenon. These results suggest that the SPB for El Niño events is closely related to the spatial structure of initial error patterns, and that a particular initial error pattern could cause a significant SPB for El Niño events. It is demonstrated that initial error patterns that have a dynamical behaviour similar to El Niño and La Niña may exhibit an apparent season-dependent evolution and cause a large prediction error, yielding a significant SPB. Two classes of CNOP-type errors possess almost the same dynamical behaviour as El Niño and La Niña and induce the largest prediction error and then can be regarded as most likely to cause a significant SPB phenomenon, an observation that encourages consideration of whether ENSO forecast skill can be greatly improved when these types of initial errors are filtered out through a data assimilation or a target approach.

The differences between CNOP and LSV reflect the effect of nonlinearities on the SPB for El Niño events.

DOI: 10.1002/qj

The results in this paper imply that the growth-phase predictions, especially for the strong El Niño events, may be affected by relatively strong nonlinearities compared to the decaying-phase predictions. The CNOP-type errors cover a broader region than the LSV-type errors. And this localized region of the CNOP-type errors with large values always arising in the equatorial central-eastern Pacific is more likely to capture the 'sensitive area' of ENSO prediction, a result that may guide efforts to intensify observations in this area and improve ENSO prediction.

This paper investigates the SPB based on model El Niño events and only considers the role of initial errors in the SPB. The results demonstrate that the occurrence of the SPB for El Niño depends on the spatial structure of the initial errors. There are some papers, which used the stochastic optimal approach to investigate ENSO predictability (Kleeman and Moore, 1997; Moore and Kleeman, 1999). In these studies, the authors explored the role of stochastic noise forcing, which, actually, emphasized the effect of a kind of model error on ENSO predictability. It is known that both initial error and model error are origins of prediction uncertainties of El Niño. However, it is unknown which kind of error plays the dominant role in causing a significant SPB for El Niño events. We therefore expect that future work can address this question. Furthermore, since the main characteristics of La Niña events (e.g. phase-locking) cannot be well-modelled by the Zebiak–Cane model (An and Wang, 2001), no attempt has been made in this paper to study the corresponding problem for La Niña events. We also anticipate that a more realistic ENSO model can be used to investigate the SPB for ENSO events for the purpose of identifying the differences in predictability of El Niño and La Niña.

The SPB for ENSO is an unresolved problem, though it has attracted the attention of plenty of scientists. This paper reveals that CNOP-type error is most likely to cause a significant SPB for El Niño and identifies the common characteristics of such errors. We also explore the effect of the different phases of El Niño on the SPB, distinguishing the different forecast skill of the growth-phase and the decaying-phase predictions for El Niño. Furthermore, we explore the role of the nonlinearities in the error growth related to the SPB, distinguishing the different amplitude of effects of nonlinearities on the SPB. As noted above, model error may also affect ENSO predictability, in which case it is uncertain whether the CNOP-type errors will necessarily exhibit the common characteristics revealed in this paper, making it vital to study the effect of model error on the SPB for ENSO events. Furthermore, realistic hindcast experiments should be conducted to apply these theoretical results and examine their reliability.

Much of the challenge in ENSO forecasting is also the avoidance of false predictions of El Niño events, which indicates that, in realistic predictions, we do not know whether an event will develop. This work is focused on the analysis of El Niño events that do occur, from the view of hindcast experiments, and suggests information on improving ENSO prediction skill. Such information as the aforementioned should be applied in realistic prediction to see how large the gap between theory and reality is. Furthermore, it is expected that a more realistic error-filtering strategy that is not conditional upon knowing whether an event will occur can be explored.

Acknowledgements

This work was jointly sponsored by the National Nature Scientific Foundation of China (Nos. 40675030; 40523001; 40830955) and the National Basic Research Program of China (Nos.2006CB403606; 2007 CB411800).

References

An S-I, Wang B. 2001. Mechanisms of locking of the El Niño and La Niña mature phases to boreal winter. *J. Climate* **14**: 2164–2176.

Birgin EG, Martínez JM, Raydan M. 2000. Nonmonotone spectral projected gradient methods on convex sets. *SIAM J. Optim.* **10**: 1196–1211.

Bjerknes J. 1969. Atmospheric teleconnections from the equatorial Pacific. *Mon. Weather Rev.* **97**: 163–172.

Blumenthal MB. 1991. Predictability of a coupled ocean–atmosphere model. *J. Climate* **4**: 766–784.

Chen D, Zebiak SE, Busalacchi AJ, Cane MA. 1995. An improved procedure for El Niño forecasting: Implications for predictability. *Science* **269**: 1699–1702.

Chen D, Cane MA, Kaplan A, Zebiak SE, Huang DJ. 2004. Predictability of El Niño over the past 148 years. *Nature* **428**: 733–736.

Duan WS, Mu M. 2006. Investigating decadal variability of El Niño–Southern Oscillation asymmetry by conditional nonlinear optimal perturbation. *J. Geophys. Res.* **111**: C07015, DOI:10.1029/2005JC003458.

Duan WS, Mu M, Wang B. 2004. Conditional nonlinear optimal perturbations as the optimal precursors for El Niño–Southern Oscillation events. *J. Geophys. Res.* **109**: D23105, DOI:10.1029/2004JD004756.

Duan WS, Xu H, Mu M. 2008. Decisive role of nonlinear temperature advection in El Niño and La Niña amplitude asymmetry. *J. Geophys. Res.* **113**: C01014, DOI:10.1029/2006JC003974.

Farrell BF. 1988. Optimal excitation of neutral Rossby waves. *J. Atmos. Sci.* **45**: 163–172.

Farrell BF, Ioannou PJ. 1996. Generalized stability theory. Part II: Nonautonomous operators. *J. Atmos. Sci.* **53**: 2041–2053.

Jin EK, Kinter III JL, Wang B, Park C-K, Kang I-S, Kirtman BP, Kug J-S, Kumar A, Luo J-J, Schemm J, Shukla J, Yamagata T. 2008. Current status of ENSO prediction skill in coupled ocean–atmosphere models. *Clim. Dyn.* **31**: 647–664.

Karspeck AR, Kaplan A, Cane MA. 2006. Predictability loss in an intermediate ENSO model due to initial error and atmospheric noise. *J. Climate* **19**: 3572–3588.

Kirtman BP, Shukla J, Balmaseda MA, Graham N, Penland C, Xue Y, Zebiak SE. 2002. '*Current status of ENSO forecast skill: A report to the Climate Variability and Predictability (CLIVAR) Numerical Experimentation Group (NEG)*'. CLIVAR Working Group on Seasonal to Interannual Prediction, Climatic Variability and Predictability, Southampton Oceanographic Centre: Southampton, UK.

Kleeman R, Moore AM. 1997. A theory for the limitation of ENSO predictability due to stochastic atmospheric transients. *J. Atmos. Sci.* **54**: 753–767.

Latif M, Barnett TP, Cane MA, Flügel M, Graham NE, von Storch H, Xu J-S, Zebiak SE. 1994. A review of ENSO prediction studies. *Clim. Dyn.* **9**: 167–179.

Lau K-M, Yang S. 1996. The Asian monsoon and predictability of the tropical ocean–atmosphere system. *Q. J. R. Meteorol. Soc.* **122**: 945–957.

Liu DC, Nocedal J. 1989. On the limited memory BFGS method for large scale optimization. *Math. Programming* **45**: 503–528.

Lorenz EN. 1965. A study of the predictability of a 28-variable atmospheric model. *Tellus* **17**: 321–333.
Luo J-J, Masson S, Behera SK, Yamagata T. 2008. Extended ENSO predictions using a fully coupled ocean–atmosphere model. *J. Climate* **21**: 84–93.
McPhaden MJ. 2003. Tropical Pacific Ocean heat content variations and ENSO persistence barriers. *Geophys. Res. Lett.* **30**: 1480, DOI:10.1029/2003GL016872.
Moore AM, Kleeman R. 1996. The dynamics of error growth and predictability in a coupled model of ENSO. *Q. J. R. Meteorol. Soc.* **122**: 1405–1446.
Moore AM, Kleeman R. 1999. Stochastic forcing of ENSO by the intraseasonal oscillation. *J. Climate* **12**: 1199–1220.
Mu M, Duan WS. 2003. A new approach to studying ENSO predictability: Conditional nonlinear optimal perturbation. *Chin. Sci. Bull.* **48**: 1045–1047.
Mu M, Zhang Z. 2006. Conditional nonlinear optimal perturbations of a two-dimensional quasigeostrophic model. *J. Atmos. Sci.* **63**: 1587–1604.
Mu M, Duan WS, Wang B. 2003. Conditional nonlinear optimal perturbation and its applications. *Nonlinear Processes in Geophys.* **10**: 493–501.
Mu M, Sun L, Dijkstra HA. 2004. The sensitivity and stability of the ocean's thermocline circulation to finite-amplitude perturbations. *J. Phys. Oceanogr.* **34**: 2305–2315.
Mu M, Duan WS, Wang B. 2007a. Season-dependent dynamics of nonlinear optimal error growth and El Niño–Southern Oscillation predictability in a theoretical model. *J. Geophys. Res.* **112**: D10113, DOI:10.1029/2005JD006981.
Mu M, Xu H, Duan WS. 2007b. A kind of initial errors related to 'spring predictability barrier' for El Niño events in Zebiak–Cane model. *Geophys. Res. Lett.* **34**: L03709, DOI:10.1029/2006GL027412.
Mu M, Zhou FF, Wang HL. 2009. A method for identifying the sensitive areas in targeted observations for tropical cyclone prediction: Conditional nonlinear optimal perturbation. *Mon. Weather Rev.* **137**: 1623–1639.
Oortwijn J, Barkmeijer J. 1995. Perturbations that optimally trigger weather regimes. *J. Atmos. Sci.* **52**: 3952–3944.
Powell MJD. 1982. '*VMCWD: A FORTRAN subroutine for constrained optimization*'. DAMTP Report 1982/NA4, University of Cambridge, UK.
Samelson RM, Tziperman E. 2001. Instability of the chaotic ENSO: The growth-phase predictability barrier. *J. Atmos. Sci.* **58**: 3613–3625.
Sun L, Mu M, Sun D-J, Yin X-Y. 2005. Passive mechanism of decadal variation of thermohaline circulation. *J. Geophys. Res.* **110**: C07025, DOI:10.1029/2005JC002897.
Terwisscha van Scheltinga AD, Dijkstra HA. 2008. Conditional nonlinear optimal perturbations of the double-gyre ocean circulation. *Nonlinear Processes in Geophys.* **15**: 727–734.
Thompson CJ. 1998. Initial conditions for optimal growth in a coupled ocean–atmospheric model of ENSO. *J. Atmos. Sci.* **55**: 537–557.
van Oldenborgh GJ, Balmaseda MA, Ferranti L, Stockdale TN, Anderson DLT. 2005. Evaluation of atmospheric fields from the ECMWF seasonal forecasts over a 15-year period. *J. Climate* **18**: 3250–3269.
Wang B, Fang Z. 1996. Chaotic oscillations of tropical climate: A dynamic system theory for ENSO. *J. Atmos. Sci.* **53**: 2786–2802.
Wang C, Picaut J. 2004. Understanding ENSO physics: A review. Earth's Climate: The Ocean–Atmosphere Interaction. *Geophys. Monogr. Amer. Geophys. Union* **147**: 21–48.
Webster PJ. 1995. The annual cycle and the predictability of the tropical coupled ocean–atmosphere system. *Meteorol. Atmos. Phys.* **56**: 33–55.
Webster PJ, Yang S. 1992. Monsoon and ENSO: Selectively interactive systems. *Q. J. R. Meteorol. Soc.* **118**: 877–926.
Wu XG, Mu M. 2009. Impact of horizontal diffusion on the nonlinear stability of thermohaline circulation in a modified box model. *J. Phys. Oceanogr.* **39**: 798–805.
Xu H, Duan WS. 2008. What kind of initial errors cause the severest prediction uncertainty of El Niño in Zebiak–Cane model. *Adv. Atmos. Sci.* **25**: 577–584.
Xue Y, Cane MA, Zebiak SE. 1997. Predictability of a coupled model of ENSO using singular vector analysis. Part I: Optimal growth in seasonal background and ENSO cycles. *Mon. Weather Rev.* **125**: 2043–2056.
Yu J-Y, Kao H-Y. 2007. Decadal changes of ENSO persistence barrier in SST and ocean heat content indices: 1958–2001. *J. Geophys. Res.* **112**: D13106, DOI:10.1029/2006JD007654.
Zebiak SE, Cane MA. 1987. A model El Niño–Southern Oscillation. *Mon. Weather Rev.* **115**: 2262–2278.